Research Article Vol. 33, No. 2 / 27 Jan 2025 / Optics Express 3429
Optics EXPRESS

Self-oscillating, self-stabilizing, and self-referenced electro-optic comb

LAWRENCE ROBERT TRASK,[1,3] SRINIVAS VARMA PERICHERLA,[2] AND PETER J. DELFYETT[1,2,4]

[1]CREOL, The College of Optics and Photonics at the University of Central Florida, 4304 Scorpius St., Orlando, Florida 32816, USA
[2]University of Central Florida, Department of Electrical and Computer Engineering, 4328 Scorpius St., Orlando, Florida 32816, USA
[3]la504684@ucf.edu
[4]delfyett@creol.ucf.edu

Abstract: We demonstrate a widely spaced, stabilized, and self-referenced opto-electronic oscillator driven electro-optic modulator based optical frequency comb. Using an ultra-stable Fabry-Perot etalon as a stable reference, we simultaneously stabilize a CW laser and generate a low noise and stable RF oscillation used to drive an electro-optic comb. In such a manner, the Fabry-Perot etalon pins both the carrier-envelope-offset frequency (f_{ceo}) and the repetition rate of the comb in place (f_{rep}), eliminating the need for an external RF oscillator. Usage of the ultra-stable Fabry-Perot etalon as both an optical and RF reference allows the removal of an external RF oscillator. Additionally, we determined the key parameters in producing high contrast ultrashort pulses necessary for coherent octave spanning supercontinuum generation using long and weak pulses associated with electro-optic modulator based combs. By using a monolithically fiber based pulse compression scheme, we produced ultrashort pulses to facilitate measuring the carrier-envelope-offset frequency, allowing for the first self-starting, self-stabilized, and self-referenced opto-electronic oscillator driven electro-optic modulator based optical frequency comb.

1. Introduction

Stabilized optical frequency combs are a powerful tool for spectroscopy [1], frequency metrology [2], astronomy [3], low noise microwave signal generation [4], and arbitrary waveform generation [5]. The optical frequency comb acts as an intermediary for synchronizing electronic frequencies with the ultrafast oscillations of optical frequencies. An optical frequency comb consists of several equidistant combines centered at an optical frequency and separated by the repetition rate, f_{rep}. The exact optical carrier frequency of each comb tooth can be determined by the simple relation $f_n = f_{ceo} + nf_{rep}$, where f_{ceo} is the optical carrier envelope offset caused by the carrier to envelope phase slippage. Measurement and control of both f_{ceo} & f_{rep} is required for knowledge of the absolute frequencies of each combline [4].

Traditional mode-locked lasers typically operate with repetition rates under 1 GHz [6], [7] while micro-ring resonators operate with repetition rates on the order of 100's of GHz to 1 THz [8]. For applications such as astro-combs and photonic assisted ADC's, repetition rates of 10 – 100 GHz are desired due to photodetector bandwidth limitations [9]. Additionally, astro-combs desire spectral uniformity to avoid saturating the detector [10]. This makes even 10 GHz micro-ring resonators difficult due to the generated spectral profile.

Due to limited availability of robust optical frequency combs with repetition rates of 10 – 100 GHz with high power per combline, alternative robust comb sources need to be explored. Electro-optic modulator (EOM) based optical frequency combs solve all of the above problems relating to robustness, high power per combline, and repetition rate. An EOM comb consists of a

#535014 https://doi.org/10.1364/OE.535014
Journal © 2025 Received 22 Jul 2024; revised 3 Jan 2025; accepted 4 Jan 2025; published 23 Jan 2025

Optics EXPRESS

CW laser and a cascade of electro-optic modulators driven by a common RF source [11]. The repetition rate of the EOM comb is determined by the RF drive frequency while fluctuations in f_{ceo} are determined by the fluctuations of in the CW laser. EOM combs exhibit square like optical spectra allowing for high power per combline. In contrast, micro-ring resonators have a limited conversion efficiency associated with the optical pump and have a sech spectral profile.

Although EOM combs solve the aforementioned issues, they are costly and difficult to self-reference due to poor pulse contrast, relatively long pulse durations, low pulse energy due to high repetition rates, and high multiplied microwave noise. Previous works such as [12] & [13] have elucidated the need for pulse conditioning, external optical filtering, and ultra low phase noise external RF sources for measuring the carrier-envelope-offset frequency. In these works, high order dispersion compensation was required to overcome the inherent higher order chirp in EOM combs.

In addition to the issues related to EOM combs (pulse energy, pulse contrast, pulse duration, and phase noise), watt level commercial optical amplifiers in the telecommunications band are not suitable for directly amplifying ultrashort pulses. Commercially available optical amplifiers that support ultrashort pulses using normal dispersion erbium doped fiber are limited to only 0.5 W of average power. Although several Watt average power EDFA's are commercially available, they exclusively employ Er/Yb doped gain fibers which are designed with anomalous dispersion. The use of anomalous dispersion gain fibers complicates the process of nonlinear pulse compression due to soliton effects [14]. Chirped pulse amplification may be employed to circumvent the soliton effects at the cost of additional complexity through pulse compression. To obtain ~nJ pulse energies required for a coherent octave for measuring f_{ceo} at a repetition rate of 10 GHz, average powers in excess of 10 W are required. To circumvent this issue, expensive waveshapers are either employed to tailor the amplitude & phase of each combline in an EOM comb [12] or apply high order dispersion [13].

It is important to note that the goal is to ensure both f_{ceo} & f_{rep} are held constant and stable. One approach to do this is to stabilize the CW laser frequency to an optical reference (such as a stable optical cavity) and use an external RF source. However, this approach uses an extra RF source and does not leverage the stability of the optical cavity to it's fullest. Alternatively, a photonically filtered optoelectronic oscillator (OEO) can be employed using the same optical cavity for stabilizing f_{ceo} to also define a f_{rep}. This allows the repetition rate to be internally generated by the etalon, eliminating the need for an external RF source and simultaneously fixing both f_{ceo} & f_{rep}. A photonically filtered OEO can be formed by photodetecting the ASE beat noise occurring at multiples of the etalon's free spectral range (FSR) and feeding the resulting photocurrent back into an intensity modulator (placed before the etalon) [15]. Photonically filtered OEOs have demonstrated enhanced environmental stability compared to their electrically filtered counterparts with low phase noise [16]. To complete the process of converting a stable CW laser into a stable comb source with both f_{ceo} & f_{rep} stabilized by a stable optical cavity, electro-optic phase modulators are driven by the same OEO signal [17]. The resulting optical bandwidth is determined by the RF drive power, RF frequency, and total accumulated modulation index of the phase modulators.

In measuring f_{ceo} a coherent octave of optical bandwidth is required for f-2f interferometry. It has been found that short pulses (sub-100 fs for highly nonlinear fiber and sub-220 fs for nonlinear waveguides) with high contrast are required to generate a coherent octave via supercontinuum generation. To this end, reduction of the temporal sidelobes in an EOM comb pulse are important to facilitate coherent octave spanning supercontinuum generation. EOM combs not only exhibit a square like spectrum (which implies a tranform limited pulse of a sinc profile) but also heightened temporal sidelobes due to high order dispersion [11]. Several works have been performed to reduce the sidelobe level of an EOM comb such as employing a time lens approach [18], cascading intensity modulators & applying pseudo linear temporal spectral phase [19], using

Optics EXPRESS

dual-drive Mach-Zehnder modulators (MZM) [20], and adjusting the bias voltage on the MZM [21]. Although these methods can reduce the sidelobe power in an EOM comb, they do not produce shorter pulses as they only act to reduce the residual chirp on the pulse. A nonlinear amplifying loop mirror (NALM) [22] can be used to completely eliminate the sidelobes and produce shorter optical pulses. A NALM consists of a fiber based sagnac interferometer with the reciprocity being broken via nonlinearity. This allows the NALM to act as an artifical ultrafast saturable absorber and nonlinearly reshape an input optical pulse. Complete nonlinear pulse shaping using nonlinear loop mirrors on EOM combs has been shown to effectively eliminate the pulse sidelobes [23]. Complete elimination of the temporal sidelobes in an EOM comb serves not only to enhance the pulse contrast but also to simplify nonlinear pulse compression by improving the spectral broadening process by self-phase modulation. This allows for an alignment free and simple nonlinear pulse compression scheme.

In this work, we seek to simplify some of the issues that have been mentioned above related to using a low phase noise RF source, higher order dispersion compensation for pulse compression, and watt level optical amplifiers. We eliminated the need for an external RF source by employing a photonically filtered opto-electronic oscillator loop. We also demonstrate a monolithically fiber-based pulse compressor which simultaneously eliminates the need for both higher order dispersion compensation, watt level optical amplifiers, and free space optics. The result is a self-oscillating, high repetition rate (~ 10.5 GHz), monolithically fiber based, self-referenced opto-electronic oscillator driven electro-optic modulator based optical frequency comb.

2. Experimental results

2.1. OEO driven EOM comb

Our OEO driven EOM comb (Fig. 1) consists of three main systems that are combined together: Pound-Drever-Hall loop, OEO loop, and EOM comb generation. A similar system can be found in [17] using the same Fabry-Perot etalon (FPE) and using fewer phase modulators. The system starts with a <7 Hz linewidth CW laser which is Pound-Drever-Hall (PDH) locked to a 100k finesse and ~1.5 GHz FSR Fabry Perot etalon (FPE) with Ultra-Low Expansion Quartz spacers. The AOM is used for fast frequency tuning while the phase modulator before the etalon is used for impressing anti-phase symmetric sidebands necessary for PDH locking. EDFAs placed before the etalon are used to compensate for losses incurred by components such as the AOM, intensity modulator, phase modulator, and coupling loss through the FPE. The optical amplifiers also serve to eliminate power fluctuations caused by the AOM using gain saturation. Employing PDH allows the f_{ceo} of our comb source to be stabilized by our ultra-high finesse etalon.

The OEO loop starts with an intensity modulator placed before the etalon and serves to define the repetition rate of our optical frequency comb. Amplified spontaneous emission noise resulting from the amplification is optically filtered by the FPE, resulting in narrow noise peaks spaced by the FSR of the etalon. The etalon throughput (10 dBm) is then amplified up to 21 dBm using a commercial semiconductor optical amplifier. The output of the SOA is then split using a 90/10 fiber coupler. The 10% branch is photodetected by a photodetector, amplified, filtered, and then sent back into the intensity modulator. The RF bandpass filter has a passband of 10 MHz centered at 7xFSR of the FPE (10.486 GHz) and is used to ensure no other multiple of the FSR can oscillate. An RF phase shifter is used to ensure a roundtrip phase of $\frac{2\pi}{\lambda}$ such that the ~10.5 GHz oscillation can occur. A 10 dB tap is used after the RF BPF and acts as RF output port for monitoring the OEO signal. A 3 dB coupler is used for supplying the RF signal to the EOM comb branch and the rest of the RF power is fed back into the intensity modulator. The RF spectrum of the OEO signal is shown in Fig. 2(a), exhibiting an SNR of 90 dB.

The EOM comb branch consists of the intensity modulator (used for the OEO loop) and 4 low v_π phase modulators placed after the FPE which are driven by the OEO loop. The 90% end of the optical coupler is used for EOM comb generation. Each of the EOM comb phase modulators

Optics EXPRESS

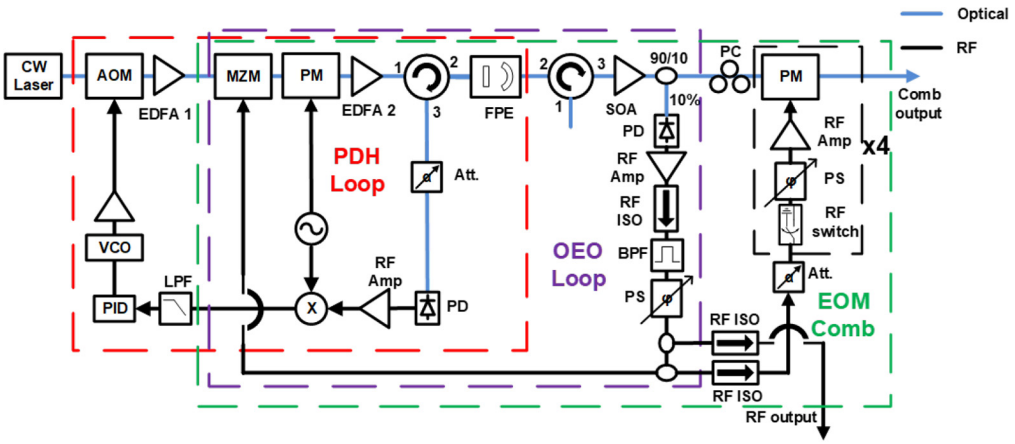

Fig. 1. OEO EOM comb schematic. AOM: acousto-optic modulator; MZM: EO intensity modulator; PM: EO phase modulator; FPE: 100k finesse Fabry-Perot etalon; SOA: semiconductor optical amplifier; PD: photodetector; BPF: RF bandpass filter; PS: RF phase shifter; LPF: low pass filter; VCO: voltage controlled oscillator.

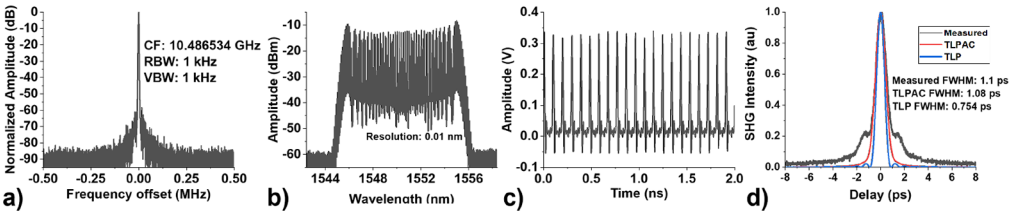

Fig. 2. OEO EOM comb data a) OEO RF spectrum, b) OEO EOM optical spectrum, c) sampling scope trace, d) intensity autocorrelation of compressed OEO EOM comb via second order dispersion (black), calculated transform limited pulse (blue), and autocorrelation of transform limited pulse (red) from OEO EOM optical spectrum .

have an RF switch, RF phase shifter, and RF amplifier (P1dB=35 dBm) to ensure maximum combline generation. The optical spectrum of the OEO EOM comb was measured directly after the final phase modulator while the sampling scope and measured intensity autocorrelation trace are measured after the EOM comb has been externally compressed using only second order dispersion. These traces are shown in Fig. 2(b), (c), and (d) respectively. The optical spectrum features 10 nm of optical bandwidth centered at 1550 nm with a flat spectral profile near the center and rabbit like ears on the edges of the spectrum. The sampling scope trace shows a clear ~10.5 GHz pulse train. The measured intensity autocorrelation trace (taken after only linear chirp compensation) shows a pulse profile with a FWHM close to the transform limit with a high pedestal. The pulse pedestal is a result of uncompensated higher order dispersion terms and can be reduced by applying the proper amount of higher order dispersion [11].

2.2. *Nonlinear pulse shaping*

From Fig. 2(d), we observe a large pulse pedestal as a result of higher order dispersion. Unfortunately, the pulse properties of the EOM comb are insufficient for coherent octave spanning supercontinuum generation which is used for measuring f_{ceo}. The target pulse parameters for coherent octave spanning supercontinuum generation in waveguides are: τ_p<220fs, E_p>200pJ, and low pulse pedestal. Our EOM comb offers pulse durations of ~600 fs (deconvolved), $E_p \sim 50pJ$ (when amplified to 0.5 W), and low pulse contrast. Higher order dispersion

Optics EXPRESS

compensation can be used to reduce the pulse pedestal but is expensive and complicated. Here, we demonstrate elimination of the pulse pedestal by means of nonlinear pulse shaping. A nonlinear amplifying loop mirror (NALM) is used as a saturable absorber to reshape the pulse spectrum into a sech and eliminate the pulse pedestal. The schematic and associated data are shown in Fig. 3.

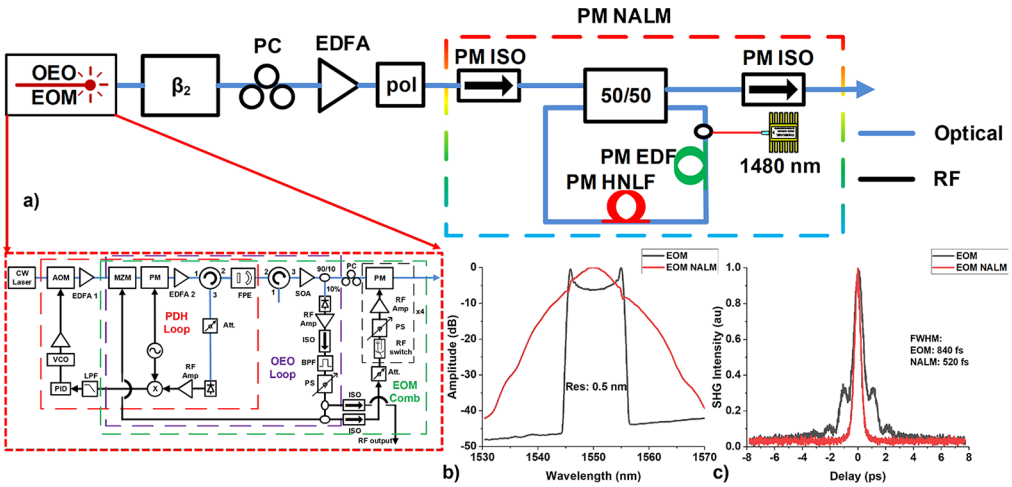

Fig. 3. Pulse pedestal suppression of the OEO EOM using a 50/50 NALM. a) schematic, b) optical spectrum, c) intensity autocorrelation.

The NALM consists of all polarization maintaining components such as PM fiber isolators, PM 50/50 coupler, PM erbium doped fiber, and 100 m of PM highly nonlinear fiber. The usage of all PM components eliminates polarization drift allowing for stable and long term operation [24]. The highly nonlinear fiber has a dispersion parameter of $D = -0.4\frac{ps}{nm \circ km}$ at 1550 nm with an elliptical core and a nonlinear coefficient $\gamma = 10.7\frac{1}{W \circ km}$. From Fig. 3, we observe a complete removal of the pulse pedestal from the original EOM comb, and the optical spectrum resembles that of a sech pulse. The intensity autocorrelation FWHM of the EOM comb has decreased from 840 fs to 520 fs while the deconvolved pusle width has decreased to ~340 fs. This clearly demonstrates the NALM's ability to simultaneously provide pulse contrast enhancement and pulse shortening.

2.3. *Pulse amplification*

Although the pulse pedestal of the EOM comb has been removed, the pulse duration is still too long for coherent octave spanning supercontinuum generation. Additionally, to reach 200 pJ of pulse energy at a repetition rate of 10 GHz, an average power of 2 W is needed. Due to the relatively high average power needed, gain narrowing, polarization fluctuations (due to higher heat load), and amplifier nonlinearities must be taken into consideration. Instead we utilize a two step amplification process to achieve ~200 pJ pulse energies using amplifiers with saturation powers less than 0.6 W. The process consists of amplification, pulse-picking, and re-amplification. We constructed a tunable external optical cavity (finesse ~200 and FSR matching f_{rep}) to reduce the noise in between comblines due to accumulated ASE and multiplied up microwave noise. The schematic and associated data for our two step amplification process is shown in Fig. 4. The output of the PM NALM is first sent into a phase modulator for impressing phase modulated sidebands necessary for locking the tunable optical cavity to our comb source. Then the pulses are pre-chirped with only second order dispersion before entering a home-made PM 0.5 W EDFA. Nonlinear spectral broadening in the PM EDFA and subsequent pulse compression from PM1550

Optics EXPRESS

fiber can be seen in Fig. 4(b) and (c), where the intensity autocorrelation FWHM has further been reduced from 520 fs to 340 fs. Additionally, we note that no noticeable pulse pedestal has formed after the spectral broadening in the amplifier.

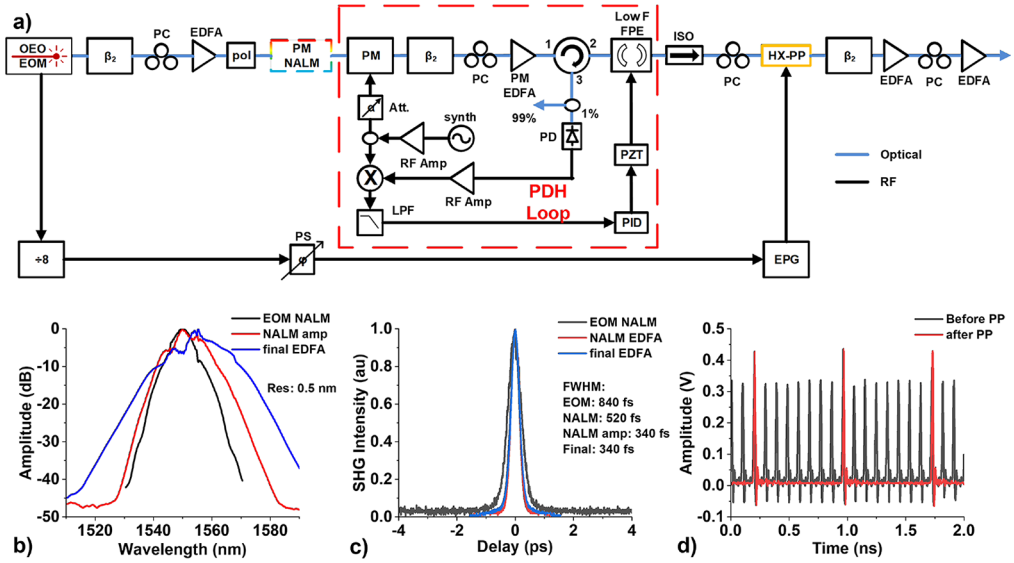

Fig. 4. Monolithically fiber based nonlinear pulse compression scheme using 50/50 NALM and nonlinear spectral broadening in EDFAs. a) schematic, b) optical spectrum, c) intensity autocorrelation, d) sampling scope.

The amplified pulses are then sent into the tunable external FPE for filtering the noise in between comblines. We measure an insertion loss of ~2.5 dB loss due to a minor mismatch in the tunable FPE's FSR and our generated comb. Despite the slight mismatch, the majority of the comb passes through with minimal change to the pulse. After optical filtering, the pulse train is downsampled by a factor of 8, reducing the repetition rate from ~10.5 GHz to ~1.3125 GHz and reducing the average power from ~300 mW to ~10 mW (pulse-picker loss and insertion loss of the pulse-picker). A sampling scope trace before & after the pulse-picker are shown in Fig. 4(d), where we clearly observe good extinction of the pulse-picking process. The pulse-picker is driven by an electrical pulse generator (FWHM: 50 ps) which is driven by the OEO signal divided by 8. After the pulse-picker, the pulses are pre-chirped again by only second order dispersion and re-amplified up to 24.2 dBm. To reduce the overall incurred ASE (keeping the total gain of a single fiber amplifier less then 20 dB), a pre-amplifier is used to provide 10 dB gain and the rest of the gain is achieved by a final home-made EDFA. The optical spectrum and intensity autocorrelation of the final EDFA are shown in Fig. 4(b) and (c). We observe a noticeable increase in the optical spectrum while the intensity autocorrelation FWHM remains the same, indicating a residual up-chirp. Previous work on studying the effect of chirping the input pulse prior to supercontinuum generation has highlighted the importance of dispersion management [25]. Although the output pulses are slightly up-chirped, the pulse duration out of the final EDFA is still within 10% of the transform limited pulse. This entails the comb-line contrast is minimally affected by the chirping of the pulse. Nonetheless, the amplified pulses are sufficient for measuring a f_{ceo} beat signal using nonlinear waveguides.

2.4. Carrier-envelope-offset detection

To measure the carrier-envelope-offset frequency of our OEO EOM comb, we used a commercial carrier-envelope-offset stabilization module (COSMO) from Octave Photonics. The COSMO

Optics EXPRESS

contains Tantala nonlinear waveguides for coherent octave spanning supercontinuum generation, periodically poled Lithium Niobate (PPLN) for second harmonic generation, and a 1 GHz photodetector with integrated transimpedance amplifier. The COSMO unit used in this work only has a single RF output and no optical output for measuring the supercontinuum generation. The RF output is fed into an RF low noise amplifier for improving the SNR of the f_{ceo} beat signal. This can be seen in Fig. 5. In Fig. 5(b), the f_{ceo} beat note can be seen centered at ~180 MHz. The noise after 800 MHz drops a few dB due to the photodetector response. Figure 5(c) shows the RF spectrum of the f_{ceo} beat note on a smaller span. We observe the beat note has a spectral width of 40 MHz FWHM and an SNR ~27 dB. We note that the width of the f_{ceo} beat note mimics that of the tunable etalon employed. This is a result of the OEO RF phase noise being above the β separation line [26]. We expect the f_{ceo} linewidth to be broadened by the same mechanism of multiplied up RF phase noise found in a typical EOM comb.

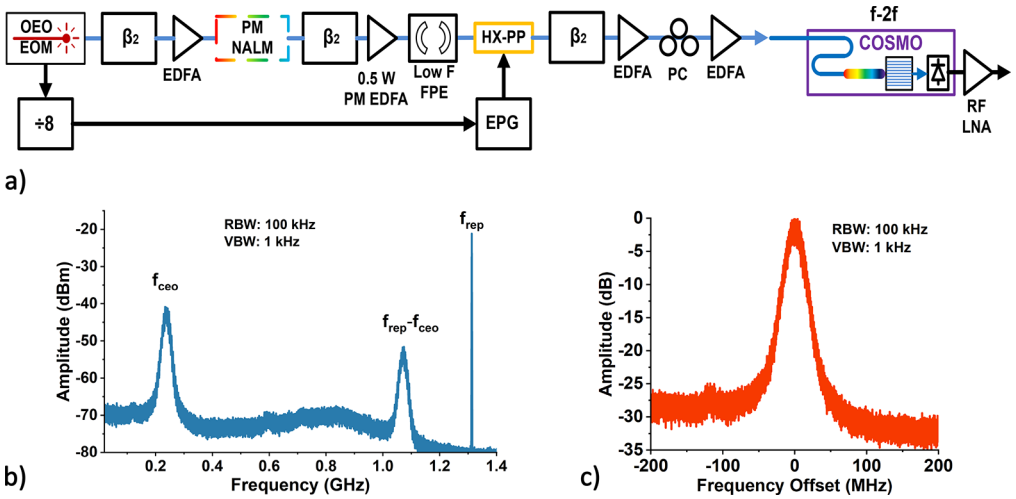

Fig. 5. Carrier-envelope-offset frequency detection of the OEO EOM OFC using monolithic fiber based pulse compressor and nonlinear waveguides for f-2f interferometry. a) schematic, b) RF spectrum (1.4 GHz span), c) RF spectrum of f_{ceo} (400 MHz span).

From Fig. 6(a), we clearly see that the OEO phase noise is above the β separation line at all frequency offsets. This indicates that the width of the f_{ceo} beat note would be primarily due to the width of the external tunable cavity employed. Methods to reduce the f_{ceo} linewidth include using a higher finesse tunable etalon to filter lower frequency offset RF phase noise and/or reducing the RF phase noise [16] of the RF source below the β separation line. The absolute timing jitter of the OEO was calculated to be 2.484 ps (1 Hz - 100 MHz), where approximately 2.1 ps of timing jitter is a result of the phase noise from 1 Hz - 10 Hz. It is important to note that although the width of the beat note is wide, the beat note does not drift. Continuous measurement of f_{ceo} was conducted over 3 hours and no change in f_{ceo} could be observed. This is a consequence of the CW laser being pre-stabilized by the optical cavity, demonstrating that our approach indeed keeps f_{ceo} & f_{rep} constant.

The measured fractional frequency stability, shown in Fig. 6(b), exhibits a small improvement in stability over our previous works. This is a result of higher power out of the etalon, higher power into the photodetector, fewer RF amplifiers in the OEO loop, and the inclusion of a ~10 MHz FWHM RF bandpass filter. State of the art 10 GHz RF oscillators, such as the sapphire loaded cavity oscillator employed in [12], exhibit a fractional frequency stability of ~ $3x10^{-13}$ at 1 s, while our free-running OEO exhibits a fractional frequency stability of ~ $2x10^{-10}$.

Optics EXPRESS

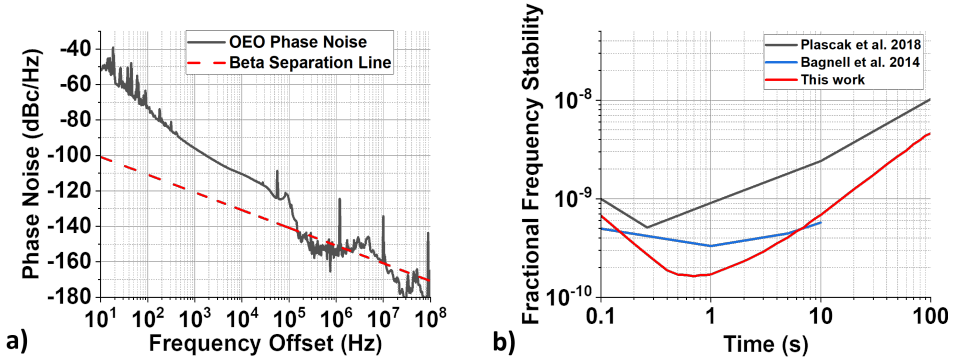

Fig. 6. Measured OEO a) RF phase noise and b) fractional frequency stability.

Further improvement of the fractional frequency stability is possible through implementing f_{ceo} stabilization in the current system.

3. Conclusion

A 10 GHz spaced, self-starting, self-stabilized, and self-referenced optoelectronic oscillator driven electro-optic modulator based optical frequency comb has been demonstrated. We replaced the external RF oscillator with an internally generated optoelectronic oscillator loop for generating a stable and low noise 10 GHz signal. Additionally, we showed a monolithically fiber-based pulse compressor which can reshape low contrast pulses into pulses sufficient for coherent octave spanning supercontinuum generation without watt class optical amplifiers. We measured the carrier-envelope-offset frequency of our OEO EOM OFC using nonlinear waveguides and demonstrated an RF SNR of ~27 dB. This represents the first time an EOM comb has been self-referenced without an external RF source.

Funding. National Science Foundation (2052701).

Acknowledgment. L.R.T. acknowledges student support from DoD SMART scholarship. The authors would also like to acknowledge Dr. Stefan Gausmann, Dr. Matthew Cooper, Caleb Dobias, Timothy Bate for helpful discussions in constructing fiber amplifiers, fiber fusion splicing, and fiber spooling.

Disclosures. The authors declare no conflicts of interest.

Data availability. Data underlying the results presented in this paper are not publicly available at this time but may be obtained from the authors upon reasonable request.

References

1. I. Coddington, W. C. Swann, and N. R. Newbury, "Coherent multiheterodyne spectroscopy using stabilized optical frequency combs," Phys. Rev. Lett. **100**(1), 013902 (2008).
2. J. Ye, H. Schnatz, and L. W. Hollberg, "Optical frequency combs: from frequency metrology to optical phase control," IEEE J. Sel. Top. Quantum Electron. **9**(4), 1041–1058 (2003).
3. R. A. McCracken, J. M. Charsley, and D. T. Reid, "A decade of astrocombs: recent advances in frequency combs for astronomy," Opt. Express **25**(13), 15058–15078 (2017).
4. T. M. Fortier, M. S. Kirchner, F. Quinlan, *et al.*, "Generation of ultrastable microwaves via optical frequency division," Nat. Photonics **5**(7), 425–429 (2011).
5. P. J. Delfyett, S. Gee, M.-T. Choi, *et al.*, "Optical frequency combs from semiconductor lasers and applications in ultrawideband signal processing and communications," J. Lightwave Technol. **24**(7), 2701–2719 (2006).
6. D. M. Lesko, A. J. Lind, N. Hoghooghi, *et al.*, "Fully phase-stabilized 1 ghz turnkey frequency comb at 1.56 μm," OSA Continuum **3**(8), 2070–2077 (2020).
7. B. R. Washburn, R. W. Fox, N. R. Newbury, *et al.*, "Fiber-laser-based frequency comb with a tunable repetition rate," Opt. Express **12**(20), 4999–5004 (2004).
8. V. Brasch, E. Lucas, J. D. Jost, *et al.*, "Self-referenced photonic chip soliton kerr frequency comb," Light: Sci. Appl. **6**(1), e16202 (2016).

Optics EXPRESS

9. T. Herr and R. A. McCracken, "Astrocombs: recent advances," IEEE Photonics Technol. Lett. **31**(23), 1890–1893 (2019).
10. M. T. Murphy, T. Udem, R. Holzwarth, *et al.*, "High-precision wavelength calibration of astronomical spectrographs with laser frequency combs," Mon. Not. R. Astron. Soc. **380**(2), 839–847 (2007).
11. A. J. Metcalf, V. Torres-Company, D. E. Leaird, *et al.*, "High-power broadly tunable electrooptic frequency comb generator," IEEE J. Select. Topics Quantum Electron. **19**(6), 231–236 (2013).
12. K. Beha, D. C. Cole, P. Del'Haye, *et al.*, "Electronic synthesis of light," Optica **4**(4), 406 (2017).
13. D. R. Carlson, D. D. Hickstein, W. Zhang, *et al.*, "Ultrafast electro-optic light with subcycle control," Science **361**(6409), 1358–1363 (2018).
14. G. P. Agrawal, "Optical pulse propagation in doped fiber amplifiers," Phys. Rev. A **44**(11), 7493–7501 (1991).
15. I. Ozdur, D. Mandridis, N. Hoghooghi, *et al.*, "Low noise optically tunable opto-electronic oscillator with fabry perot etalon," J. Lightwave Technol. **28**(21), 3100–3106 (2010).
16. M. Bagnell, J. Davila-Rodriguez, and P. J. Delfyett, "Millimeter-wave generation in an optoelectronic oscillator using an ultrahigh finesse etalon as a photonic filter," J. Lightwave Technol. **32**(6), 1063–1067 (2014).
17. M. E. Plascak, R. B. Ramirez, K. Bagnell, *et al.*, "Tunable broadband electro-optic comb generation using an optically filtered optoelectronic oscillator," IEEE Photonics Technol. Lett. **30**(4), 335–338 (2018).
18. Y. Xing, Q. Wang, L. Huo, *et al.*, "Frequency chirp linearization for ultraflat optical frequency comb generation based on group velocity dispersion," Opt. Lett. **38**(13), 2188–2190 (2013).
19. R. Wu, V. Supradeepa, C. M. Long, *et al.*, "Generation of very flat optical frequency combs from continuous-wave lasers using cascaded intensity and phase modulators driven by tailored radio frequency waveforms," Opt. Lett. **35**(19), 3234–3236 (2010).
20. K. Qu, S. Zhao, X. Li, *et al.*, "Ultra-flat and broadband optical frequency comb generator via a single mach–zehnder modulator," IEEE Photonics Technol. Lett. **29**(2), 255–258 (2017).
21. Y. Dou, H. Zhang, and M. Yao, "Improvement of flatness of optical frequency comb based on nonlinear effect of intensity modulator," Opt. Lett. **36**(14), 2749–2751 (2011).
22. M. E. Fermann, F. Haberl, M. Hofer, *et al.*, "Nonlinear amplifying loop mirror," Opt. Lett. **15**(13), 752–754 (1990).
23. V. Ataie, E. Temprana, L. Liu, *et al.*, "Ultrahigh count coherent wdm channels transmission using optical parametric comb-based frequency synthesizer," J. Lightwave Technol. **33**(3), 694–699 (2015).
24. K. Tamura and M. Nakazawa, "A polarization-maintaining pedestal-free femtosecond pulse compressor incorporating an ultrafast dispersion-imbalanced nonlinear optical loop mirror," IEEE Photonics Technol. Lett. **13**(5), 526–528 (2001).
25. K. L. Corwin, N. R. Newbury, J. M. Dudley, *et al.*, "Fundamental noise limitations to supercontinuum generation in microstructure fiber," Phys. Rev. Lett. **90**(11), 113904 (2003).
26. G. Di Domenico, S. Schilt, and P. Thomann, "Simple approach to the relation between laser frequency noise and laser line shape," Appl. Opt. **49**(25), 4801–4807 (2010).